Fto in the hippocampus mediates depression-like behaviors

Shu Liu
Institute of Basic Medical Sciences Chinese Academy of Medical Sciences
Jianbo Xiu
State Key Laboratory of Medical Molecular Biology, Institute of Basic Medical Sciences Chinese Academy of Medical Sciences, School of Basic Medicine Peking Union Medical College
Caiyun Zhu
State Key Laboratory of Medical Molecular Biology, Institute of Basic Medical Sciences Chinese Academy of Medical Sciences, School of Basic Medicine Peking Union Medical College
Chen Li
State Key Laboratory of Medical Molecular Biology, Institute of Basic Medical Sciences Chinese Academy of Medical Sciences, School of Basic Medicine Peking Union Medical College
Kexin Meng
State Key Laboratory of Medical Molecular Biology, Institute of Basic Medical Sciences Chinese Academy of Medical Sciences, School of Basic Medicine Peking Union Medical College
Tingfu Du
State Key Laboratory of Medical Molecular Biology, Institute of Basic Medical Sciences Chinese Academy of Medical Sciences, School of Basic Medicine Peking Union Medical College
Rongrong Han
Institute of Basic Medical Sciences Chinese Academy of Medical Sciences
Lanlan Li
State Key Laboratory of Medical Molecular Biology, Institute of Basic Medical Sciences Chinese Academy of Medical Sciences, School of Basic Medicine Peking Union Medical College
Lingdan Xu
State Key Laboratory of Medical Molecular Biology, Institute of Basic Medical Sciences Chinese Academy of Medical Sciences, School of Basic Medicine Peking Union Medical College
Yan Shen
Institute of Basic Medical Sciences Chinese Academy of Medical Sciences
Qi Xu (qixu@vip.sina.com)
State Key Laboratory of Medical Molecular Biology, Institute of Basic Medical Sciences Chinese Academy of Medical Sciences, School of Basic Medicine Peking Union Medical College

Article

Keywords: FTO, depressive symptoms, MDD

Posted Date: February 17th, 2021

DOI: https://doi.org/10.21203/rs.3.rs-194104/v1

Version of Record: A version of this preprint was published at Nature Communications on November 26th, 2021. See the published version at https://doi.org/10.1038/s41467-021-27044-7.

Abstract

Dynamic and reversible RNA methylation has emerged as a new layer of epigenetic regulation of behaviors such as learning and memory; however, whether RNA methylation plays a critical role in the pathophysiology of depression is unclear. Here, we report that expression of the fat mass and obesity associated gene (FTO), a primary RNA demethylase, is downregulated in the hippocampi of both major depressive disorder (MDD) patients and mouse models of depression. Suppressing *Fto* expression in the hippocampus induces depression-like behaviors in mice, while elevating its expression leads to antidepressant effects. Epitranscriptomic profiling of N6-methyladenosine (m^6A) RNA methylation in the hippocampi of *Fto* knockdown (KD), *Fto* knockout (cKO), and *Fto*-overexpressing (OE) mice identified adrenoceptor beta 2 (*Adrb2*) mRNA as a target of Fto. Adrb2 stimulation reverses the depression-like behaviors and spine loss induced by hippocampal Fto deficiency, possibly via the modulation of hippocampal Sirt1 expression by c-Myc. These findings reveal that Fto in the hippocampus mediates depression-like behaviors and highlight the importance of reversible RNA methylation in driving depression.

Background

Major depressive disorder (MDD) is currently the leading cause of disability worldwide and is characterized by low mood, diminished interests, feelings of despair or guilt, impaired cognition and other symptoms[1]. Epigenetic regulation of genes induced by environment interactions strongly contributes to the pathophysiology of depression[2]. Considerable progress in the understanding of DNA methylation and histone modifications has been made[3]; however, the epitranscriptomic influences on depression remain largely elusive.

N6-methyladenosine (m^6A) methylation, as the most abundant internal modification of eukaryotic mRNA, occurs extensively in the brain[4,5] and is dynamic and reversible in the mammal[6]. FTO is a well-characterized RNA demethylase that is expressed at the highest levels in multiple brain regions[7]. Previous studies have demonstrated that Fto in the brain regulates postnatal growth of mice[8], the activity of the dopaminergic midbrain circuitry[9], memory processes in the prefrontal cortex[10] and the hippocampus[11-14], brain development[12], adult neurogenesis[12], axonal regeneration[15], and localized mRNA translation[16,17]. Genetic studies have revealed that FTO is associated with depressive symptoms[18-20] and other studies have also showed FTO involve in the pathogenesis of MDD[11,21]. These studies showed that FTO may play a vital role in MDD, however, the specific role of FTO in mediating depression-like behaviors and the underlying mechanisms have yet to be clarified.

Results

FTO expression is downregulated in the hippocampi of MDD patients and mouse models of depression

We performed microarray analysis of the peripheral blood of 36 MDD patients and 20 healthy controls, and found that both RNA methyltransferases (*METTL3*, *METTL14*, and *WTAP*) and demethylases (*FTO* and *ALKBH5*) were significantly downregulated in MDD (Fig. 1a). We further measured the expression of m^6A-modifying enzymes in three mouse models of depression, including the chronic unpredictable mild stress (CUMS), chronic restraint stress (CRS), and social defeat stress (SDS) models, which are widely employed in preclinical studies of depression. In CUMS model mice, the mRNA expression of *Fto* and *Alkbh5* in the peripheral blood was significantly downregulated compared to that in control mice, whereas the expression of RNA methyltransferases remained unchanged (Fig. 1b). Behavioral tests showed that all three models of depression were successfully established (Fig. 1c, d, g, h, k, and l). We examined the mRNA expression of m^6A-modifying enzymes in multiple brain regions involved in regulating emotion, including the prefrontal cortex (PFC), nucleus accumbens (NAC), amygdala (AMY), and hippocampus (HIP). We found that *Fto* was consistently downregulated in the hippocampi of all three animal models compared to the hippocampi of control mice (Fig. 1e, i, m), whereas there was either no change or inconsistent changes in the expression of the other examined enzymes (Supplementary Fig. 1a-c). Western blot analysis further confirmed that Fto was significantly downregulated in the hippocampi of all three mouse models compared to the hippocampi of control mice (Fig. 1f, j, n). Postmortem study revealed that mRNA expression of *FTO* was specifically and significantly decreased in the hippocampi of MDD patients compared to healthy controls (Fig. 1o, Supplementary Table 1).

Fto mediates depression-like behaviors in the hippocampus

To test how hippocampal Fto contributes to depression-like behaviors, we employed recombinant adeno-associated virus (rAAV) as a transgenic tool to specifically knock down and overexpress mouse *Fto* in the hippocampi of wild-type C57BL/6 mice and to specifically knock out *Fto* in the hippocampi of *Fto* flox/flox mice. Four weeks after bilateral microinjection of rAAV into the hippocampus (Fig. 2a), *Fto* protein expression was manipulated as expected in shRNA-expressing (knockdown; KD), *Fto*-overexpressing (OE), and Cre-expressing (cKO) mice (Fig. 2b). As Fto catalyzes RNA demethylation, the m^6A dot blot assay showed that altering the expression level of Fto increased m^6A levels in hippocampal total RNA from KD and cKO mice and decreased m^6A levels in hippocampal total RNA from OE mice (Fig. 2c). Next, we analyzed the behavioral consequences of changes in *Fto* expression. KD mice demonstrated a longer immobility duration in the tail suspension test (TST) and a lower sucrose preference in the sucrose preference test (SPT) than control mice (Fig. 2d, e). cKO mice showed longer immobility durations in the TST and the forced swimming test (FST) as well as a longer latency to feed in the novelty suppressed feeding test (NSFT) than EGFP-expressing mice (Fig. 2f, g, h). These results reveal that suppressing *Fto* expression in the hippocampus is sufficient to induce depression-like behaviors in mice. Subsequently, we asked whether overexpression of *Fto* leads to antidepressant effects. CUMS induced depression-like behaviors in EGFP-expressing mice; however, stress-treated OE mice demonstrated a shorter immobility duration in the TST and a higher sucrose preference in the SPT than

CUMS-treated EGFP-expressing mice (Fig. 2i-k). These results reveal that overexpression of *Fto* in the hippocampus has antidepressant effects.

Recent studies have reported various effects of systemic *Fto* knockout on anxiety-like behaviors in mice[13,21]. Owing to the high comorbidity of depression and anxiety, we also analyzed the anxiety-like behaviors of KD and cKO mice. There was no significant difference in the time spent in the center zone in the open field test (OFT) between KD and control mice (Supplementary Fig. 2a). Additionally, in the elevated zero maze test (EZM), there was no significant difference in the time spent in the open arms between KD and control mice (Supplementary Fig. 2b). Similar results were observed for cKO mice (Supplementary Fig. 2c, d). These results are consistent with a previous study that used a specific Cre line to knock out *Fto* in the CA1 and CA3 regions of the hippocampus[11]. Our study demonstrates that Fto in the hippocampus specifically mediates depression-like behaviors without affecting anxiety-like behaviors. Specific deletion of *Fto* in the nervous system results in postnatal growth retardation[8]; therefore, we asked whether the depression-like phenotype observed in cKO mice is due to abnormal growth. However, there was no significant difference in body weight between control and cKO mice, indicating that downregulation of *Fto* in the hippocampus does not affect growth (Supplementary Fig. 3a). Moreover, after 24 hours of food deprivation, there were no changes in body weight between the two groups of mice (Supplementary Fig. 3b, c).

Modification of the hippocampal m^{6}A epitranscriptome by Fto

How does hippocampal Fto mediate depression-like behaviors? We aimed to answer this question by performing m^{6}A epitranscriptomic analysis of hippocampal mRNAs by MeRIP-Seq. After quality control, 47.01 to 76.53 million reads were generated from each m^{6}A-seq library. An average of 88.59% reads were uniquely mapped to the mouse genome and retained for further analysis (Supplementary Table 2). Approximately 25% - 34% of the expressed genes were modified by m^{6}A, with approximately 2.65 peaks per gene. The pattern of m^{6}A modification distribution on genes was similar among groups (Supplementary Fig. 4a). Consistent with previous studies[5,22], the majority of m^{6}A peaks were preferentially located on the 3'UTR and around the stop codon, and the enriched motifs in all samples contained 'GGAC', one of the most frequent m^{6}A consensus motifs (Fig. 3a).

Next, we analyzed the differentially methylated peaks (DMPs) among different groups (Fig. 3b). Most DMPs were distributed in exons and the 3'UTR (Supplementary Fig. 4b). KEGG pathway analysis showed that multiple gene clusters were enriched in Wnt, calcium, Notch, and axon guidance signaling pathways (Fig. 3c). Specifically, hypermethylated genes in cKO mice and hypomethylated genes in OE mice were both enriched in the neuroactive ligand-receptor interaction pathway. GO analysis demonstrated that genes with hypomethylated peaks in OE mice were mostly enriched in pathways regulating synapse organization and signal release, neurotransmitter secretion and transport, and neural precursor cell proliferation (Fig. 3d).

Adrb2 is functionally important target gene of FTO in the hippocampus

As Fto is a well-characterized RNA demethylase, we analyzed both hypermethylated mRNAs in KD and cKO mice and hypomethylated mRNAs in OE mice (Fig. 4a). After mapping each peak to the corresponding gene, we found that 382 and 661 genes were hypermethylated in KD and cKO mice, respectively, while there were 613 hypomethylated genes in OE mice (Fig. 4b). Finally, we identified 34 genes that were both hypermethylated in KD and cKO mice and hypomethylated in OE mice (Fig. 4c; Supplementary Table 3). Gene-specific m^6A qPCR analysis of *Zfp217* and *Ahnak* confirmed the MeRIP-Seq results (Supplementary Fig. 4c). At the mRNA level, *Zfp217* and *Ahnak* were downregulated in cKO mice and upregulated in OE mice compared to control mice (Supplementary Fig. 4d). Among these 34 genes, *Adrb2* encodes the β2-adrenergic receptor, which has been reported to regulate synaptic plasticity, adult neurogenesis, and neuroinflammation in the hippocampus and to exert antidepressant effects[23-27]. Therefore, we wondered whether Adrb2 contributes to Fto-mediated depression-like behaviors in the hippocampus. First, we confirmed that suppressing *Fto* expression hyper-methylates *Adrb2* mRNA in KD and cKO mice and that *Fto* overexpression leads to hypomethylation of *Adrb2* mRNA in OE mice (Fig. 4d, g, j). At both the mRNA and protein levels, *Adrb2* was downregulated in KD and cKO mice but upregulated in OE mice compared to control mice (Fig. 4e, h, k, f, i, and l). Postmortem study revealed that mRNA expression of *ADRB2* was significantly decreased in the hippocampi of MDD patients compared to healthy controls (Fig. 4m). We further investigated whether changes in m^6A methylation affect *Adrb2* mRNA levels in Neuro-2a cells. In the presence of actinomycin D, an inhibitor of mRNA transcription, *Fto* knockdown accelerated the degradation of *Adrb2* mRNA, whereas *Fto* overexpression significantly delayed this process (Fig. 4n, o). When Ythdf2, an m^6A reader protein that regulates RNA stability[28], was knocked down, the level of *Adrb2* mRNA significantly increased (Fig. 4p). These results indicate that m^6A modification affects the level of *Adrb2* mRNA, at least partly by regulating its stability.

Adrb2 stimulation reverses the depression-like behaviors and spine loss induced by hippocampal Fto deficiency

We investigated whether Adrb2 contributes to the phenotype induced by hippocampal Fto deficiency. We tested this role of Adrb2 in cKO mice by stimulating Adrb2 with formoterol (FOR), a specific Adrb2 agonist that can cross the blood-brain barrier (Fig. 5a). FOR administration rescued the depression-like behaviors of cKO mice in both the FST and TST in two cohorts of mice, while pretreatment with ICI 118,551 (ICI), a specific Adrb2 antagonist, blocked the effects of FOR (Fig. 5b, c). Depression has been demonstrated to be associated with synaptic dysfunction in multiple brain regions, including the hippocampus[29]. Treatment of cKO mice with FOR for 7 consecutive days significantly increased the number of spines to a level comparable to that in EGFP-expressing mice, whereas pretreatment with ICI blocked the effects of FOR (Fig. 5d).

Adrb2 mediates depression-like behaviors possibly via the modulation of hippocampal Sirt1 expression by c-Myc

Sirt1, an NAD^+-dependent deacetylase, is essential for synaptic plasticity in the hippocampus[30,31], and it has been reported that hippocampal Sirt1 signaling mediates depression-like behaviors[32]. In our study,

the Sirt1 protein was downregulated in the hippocampi of cKO mice but upregulated in OE mice (Fig. 5e). However, in all three m^{6}A-seq libraries, we detected no change in the m^{6}A level on *Sirt1* mRNA, suggesting that Fto may regulate the expression of Sirt1 through other pathways. Recent studies have reported that Adrb2 activation upregulates Sirt1 expression in cervical cancer cells through promoting the expression of c-Myc[33]. In vitro, c-Myc can bind to the *Sirt1* promoter and induce *Sirt1* expression[34]. Thus, we wondered whether Adrb2 exerts a similar effect in the hippocampus. Blocking Adrb2 significantly decreased Sirt1 protein levels in the hippocampi of wild-type mice after i.p. administration of ICI (Fig. 5f). FOR treatment obviously increased Sirt1 expression in cKO mice compared to saline-treated cKO mice, while pretreatment with ICI blocked the effects of FOR (Fig. 5g). Similar results as those observed for Sirt1 were found for c-Myc in OE or cKO mice (Fig. 5h). There was also no change in the m^{6}A level on c-Myc mRNA in the KD, cKO, and OE m^{6}A-seq libraries. FOR treatment also obviously increased c-Myc expression in cKO mice compared to saline-treated cKO mice, while pretreatment with ICI blocked the effects of FOR (Fig. 5g). Stimulation of Adrb2 by FOR significantly increased c-Myc protein expression in wild-type mice compared to saline-treated mice, and this effect was blocked by pretreatment with ICI (Fig. 5i). Finally, overexpression of Sirt1 in the hippocampi of cKO mice effectively reversed the depression-like behaviors induced by Fto deficiency (Fig. 5j-m). These results suggest that Adrb2 acts downstream of Fto in the hippocampus to mediate depression-like behaviors and that Adrb2 may target Sirt1 through modulating the expression of c-Myc.

Discussion

Our data reveal that the expression of hippocampal FTO is decreased in both MDD patients and three mouse models of depression. Specific knockdown or knockout of *Fto* in the hippocampus induces depression-like behaviors, whereas overexpressing *Fto* has antidepressant effects. Epitranscriptomic analysis identified *Adrb2* as one of the targets modified by Fto. Loss of Fto in the hippocampus decreases the expression of Adrb2 by elevating m^{6}A level in Adrb2 mRNA. Conversely, overexpression of Fto increases the expression of Adrb2 by reducing m^{6}A level in Adrb2 mRNA. Adrb2 stimulation can rescue depressive-like behaviors and spine loss caused by hippocampal Fto deficiency and this effect can be reversed by Adrb2 inhibition, which may act via c-Myc to modulate hippocampal Sirt1 expression (Fig. 6).

Genetic studies show that the *FTO* rs9939609 variant exerts a protective effect against depression[19], and further analysis reveals that this positive association is driven by an atypical MDD subtype[18]. However, how Fto functions in the pathophysiology of depression and the roles it plays remain largely unknown. Inconsistent results regarding anxiety phenotypes found in different *Fto* mutant mice[11,13,21] highlight the regional specificity of the functions of Fto in the brain, such as modulation of dopaminergic signaling in the midbrain and regulation of fear memory in the prefrontal cortex. We found that Fto in the hippocampus is critical in mediating depression-like behaviors.

Adrb2 is an important target gene of FTO through MeRIP-seq assay and functional studies. Although FTO may target many mRNAs, our study focused on Adrb2 mRNA because Adrb2 can regulate synaptic plasticity and contribute to many mental disorders[24–26, 35]. Previous studies have reported that stimulation of central beta 2 -adrenergic receptors can produce antidepressant-like effects on behaviors of animals[36]. While a large of number of studies indicates that activation of central Adrb2 can produce antidepressant-like effects on animals, the specific mechanisms remain unclear. In our study, we found that depleted expression of Fto increases m6A levels at 3'UTRs, which in turn leads to the upregulation of Adrb2 at the RNA and the protein level. Conversely, m6A level was decreased in the hippocampal tissues of Fto overexpression and the expression of Adrb2 was increased. Wang et.al reported that m6A-containing mRNA intends to be less stable because such mRNA can be relocalized to the decay sites by YTHDF2[28]. Our results showed that Fto knockdown can accelerate the degradation of *Adrb2* mRNA, and overexpression of FTO can alleviate the degradation of *Adrb2* mRNA. Taken together, the above results revealed that FTO regulates the expression of Adrb2 relying on demethylase activity to a certain extent.

Two loci, one of which is near the *SIRT1* gene, were identified as the first robust links between genetics and depression at the whole-genome level[37]. Recent studies reported the expression of Sirt1 is significantly less in MDD patients compared to healthy subjects in the peripheral blood[38], which is consistent with our microarray analysis (in house data). Animal studies also show that Sirt1 regulates depression-like behaviors in several brain regions, including the hippocampus[32,39–41]. We observed that the methylation level of *Sirt1* mRNA is not modified by Fto; however, the protein expression of *Sirt1* is altered by Fto. Chen et al found that the expression of Sirt1 can be upregulated through activating Adrb2 through elevating c-Myc expression in cervical cancer cells[33]. c-Myc is reported to be a transcriptional factor of Sirt1 and can regulate the expression of Sirt1 in vitro[42]. Consistent with previous results, we found that injection of FOR can increase the expression of c-Myc protein in the hippocampus and injection of ICI can blocked this effect. In addition, the expression of c-Myc protein was decreased or increased in the hippocampus of FTO knockout or overexpression. For the first time, we report that Adrb2 regulates *Sirt1* expression in vivo in the hippocampi of wild-type and Fto-deficient mice. Both Adrb2 activation and elevation of hippocampal Sirt1 levels reverse the depression-like behaviors induced by Fto deficiency, suggesting that Fto may target *Sirt1* through modifying the methylation of *Adrb2* mRNA.

This study indicates that Fto in the hippocampus mediates depression-like behaviors and might be a new potential target for depression therapy. Recently developed specific FTO inhibitors show promise for treating cancer[43] and obesity[44]. Our findings also suggest that based on evidence from several weight-loss drugs[45], attention should be paid to potential adverse psychiatric events during systematic administration of FTO inhibitors.

Methods

Human subjects

Thirty-six unrelated MDD patients (20 females and 16 males) aged 39.9 ± 12.5 (SD) years and twenty unrelated healthy subjects (10 females and 10 males) aged 36.6 ± 11.1 (SD) years were recruited from the DBPR (manuscript NCOMMS-21-04052). All subjects provided written informed consent prior to participating in this study, which was approved by the Ethics Committee of the DBPR (manuscript NCOMMS-21-04052). None of the MDD patients or healthy controls had taken any psychotropic medications within 4 weeks. All patients were clinically diagnosed by at least two psychiatrists according to the Diagnostic and Statistical Manual of Mental Disorders Fourth Edition (DSM-IV) criteria and the 17-item Hamilton Rating Scale for Depression (HAMD-17). Hippocampal tissues of the human brain were provided by the Human Brain Bank, DBPR (manuscript NCOMMS-21-04052). The postmortem intervals between the death of donors and brain collection were less than 40 h, and detailed information on the donors is provided in Supplementary Table 1.

Microarray

Total blood RNA was isolated with a PAXgene Blood RNA Kit (Qiagen, 762174). The optical density values at 260/280 were approximately 1.9-2.0, and the quality of the RNA was also confirmed with an Agilent 2100 (Agilent Technologies, Santa Clara, CA). RNA samples underwent reverse transcription to synthesize double-stranded complementary DNA (cDNA), and the cDNA was then transcribed into cRNA in vitro. The cRNA was then reverse-transcribed into cDNA. The cDNA was fluorescently labeled and hybridized using a 4 × 180K lncRNA+mRNA Human Gene Expression Microarray V3.0 (CapitalBio Technology, Beijing, China). Agilent Feature Extraction (v10.7) software (Santa Clara, CA, USA) was used to analyze the hybridization map and extract the data. The chip fluorescence scanning images were saved as DAT files for analysis by the Agilent G2565CA Microarray Scanner. The data normalization and difference analysis were performed with Agilent GeneSpring software. Two groups of sample data underwent a t-test analysis to obtain the corrected P-values and fold change values. The microarray data were validated by qPCR, and the results for this microarray data have not been published. The expression of genes encoding RNA methylation-modifying enzymes was derived from the microarray data (in house data).

Animals

C57BL/6J mice at the age of 4-6 weeks were purchased from DBPR (manuscript NCOMMS-21-04052) and bred for 4-5 weeks to perform experiments. C57BL/6J, *Fto*$^{fl/fl}$ mice (Stock No. 027830) were provided by the Jackson Laboratory. These mice possess loxP sites on either side of exon 3 of *Fto*. Removal of the floxed sequence by Cre recombinase creates a null *Fto* allele. Mice were housed under a 12-h light/dark cycle at 23 ± 2 °C. All animal work was in accordance with the institutional guidelines of the Beijing Administration Office of Laboratory Animals and approved by the DBPR (manuscript NCOMMS-21-04052). This study was approved by the DBPR (manuscript NCOMMS-21-04052).

Cell culture

The Neuro-2a cell line, which was provided by the Cell Resource Center (IBMS, CAMS/PUMC), was cultured in DMEM supplemented with 10% heat-inactivated fetal bovine serum (04-001-1A, Biological Industries), 100 U/ml penicillin and 100 μg/ml streptomycin at 37 °C in 5% CO_2. Plasmids were transfected into Neuro-2a cells with Neofect™ DNA transfection reagent (TF201201, China). siRNA targeting Ythdf2 (sc-155424, Santa Cruz) was transfected into Neuro-2a cells with RNAi MAX (13778150, Thermo).

Drug administration

Formoterol (F9552, Sigma) and ICI 118,551 (HY-13951, MedChemExpress) were diluted in saline and administered via i.p. at dosages of 2 mg/kg and 10 mg/kg, respectively. To block the effects of formoterol, ICI 118,551 was administered 30 min before formoterol.

Mouse models of depression

Chronic unpredictable mild stress (CUMS). The CUMS model was established referring to a previous work[46]. Animals were subjected to 11 stressors at random for 35 days (three stressors per day from 1 to 21 d and two stressors per day from 22 to 35 d), which included a hot plate (45 °C/10 min), leaving the lights on overnight, turning the lights off in the daytime, bedding deprivation overnight, crowding (12 h), swimming stress (16 °C/3 min), food and water deprivation (12 h), wet bedding (12 h), an elevated platform (30 min), tilting of the cage at 45 degrees (12 h), and restraint stress (1 h).

Chronic restraint stress (CRS). CRS exposure was performed as previously described[47]. Mice were placed in polypropylene conical tubes (50 ml) with pores at the bottom enabling air flow. Animals had no access to food and water during restraint stress. Four hours later, the mice were returned to their home cages. The same stressor was administered once at a random time each day, which was continued for 21 days.

Social defeat stress (SDS). Social defeat stress exposure was performed according to the published protocol[48]. Briefly, C57BL/6J mice were placed into a cage in the presence of CD-1 aggressor mice for 5-10 min per day for 10 consecutive days. Then, the C57BL/6J and CD-1 mice were separated by a perforated Plexiglas plate for 24 h, which blocked all physical contact. Each C57BL/6J mouse was exposed to different CD-1 mice every day.

Behavioral test

Animals were transported and acclimated to the testing room 1 h before each behavioral test.

Forced swimming test (FST). Mice were individually placed in a beaker (height: 19 cm; diameter: 14 cm) containing 14 cm of water (23 ± 2 °C). The total test duration was 6 min. The process was videotaped, and the immobility time in the last 4 min was scored by an experienced observer who did not know the experimental treatment. Floating or only slight movement to maintain balance was considered immobility.

Tail suspension test (TST). The TST was performed with tail suspension hardware (Med Associates, USA). The mouse was suspended by its tail with a short adhesive tape connected to a load cell that transmits a signal corresponding to activity. The total test time was 6 min. After setting a lower threshold, the duration of immobility was recorded and analyzed by tail suspension software (SOF-821, Med Associates).

Sucrose consumption test (SCT). Mice were acclimatized to 1% sucrose solution for 48 h before the test. Then, each mouse was individually housed and deprived of water for 12 h. SCT was performed for 1 h, in which the amount of the 1% sucrose solution consumed was recorded.

Sucrose preference test (SPT). Mice were acclimatized to two-bottle drinking (one bottle contained water, and the other contained a 1.5% sucrose solution) for 48 h, during which the position of each bottle was switched at 24 h. Then, the mice were deprived of drinking water for 24 h. SPT was performed by providing the mice once again with two bottles for drinking for 2 h, during which the position of each bottle was switched after 1 h. The ratio of the sucrose solution consumed to the total fluid intake in the SPT was determined as the sucrose preference.

Social interaction test (SIT). The SIT was performed according to a previous report. It consists of two 2.5 min phases: the first is performed without a CD-1 mouse, and the second is performed with a CD-1 mouse. The two phases were separated by a pause of 30 sec. In both phases, the C57BL/6J mouse was placed into the rear corner of the open field opposite the wire-mesh compartment. The time spent in the interaction zone (14 cm × 24 cm) was recorded and analyzed by the EthoVision video tracking system (Noldus, the Netherlands). The social interaction ratio was calculated as the time spent in the interaction zone in the presence of the CD-1 mouse to the time spent in the absence of a CD-1 mouse. Brains of susceptible and control mice were harvested for gene expression analysis.

Novel suppressed feeding test (NSFT). We performed the NSFT by referring to a previous study. Mice were deprived of food for 24 h. During the NSFT, each mouse was placed into the corner of a square chamber (50 cm × 50 cm× 20 cm) opposite a food pellet that was placed in the center of the chamber. The latency to start eating the pellet was recorded. If the mouse did not eat the pellet within 6 min, the latency was recorded as 6 min.

Open field test (OFT). Each mouse was individually placed in one corner of a square Plexiglas box (50 cm × 50 cm × 40 cm) in a brightly lit room, allowing for free exploration of the open field arena for 10 min. The time spent in the center area of the box (12.5 cm × 12.5 cm) and the distance traveled in the box during the testing period were recorded and analyzed by the EthoVision video tracking system (Noldus, the Netherlands).

Elevated zero maze test (EZM). The EZM was performed in a circular elevated maze with two open and two enclosed arms (height: 43.5 cm; diameter: 45 cm; track width: 6.5 cm). Each mouse was individually placed in the cross area of the maze facing the closed arms and allowed to freely explore the maze for 5

min. The time spent in the open arms and the distance traveled in the maze were recorded and analyzed by the EthoVision video tracking system (Noldus, the Netherlands).

Vector construction, rAAV packaging and administration

The mouse *Fto* and *Sirt1* cDNAs were cloned into the rAAV expression vector with a CAG promoter. The *Fto* shRNA targeting 5'-GCAGCTGAAATACCCTAAACT -3' was cloned into the rAAV expression vector with a U6 promoter. AAV-CAG-Fto-2A-EGFP (Cat. # AAV2/9-XT071), AAV-CAG-Sirt1 (Cat. # AAV2/9-XT393), AAV-U6-*Fto* shRNA-CMV-ZsGreen (Cat. # AAV2/9-XT071), AAV-CMV-bGlobin-Cre-eGFP (Cat. # AAV2/9-S0231-9-H50), and AAV-CMV-bGlobin-eGFP-WPRE (Cat. # AAV2/9-S0263-9-H50) were packaged by Taitool Bioscience (Shanghai Taitool Bioscience Co.Ltd., China). The final titer of each rAAV was 3×1012 - 4×1012 vector genome (v.g.)/ml.

RNA preparation for quantitative real-time PCR

Total RNA from the hippocampus was extracted using TRIzol (Thermo Fisher Scientific, USA) according to the manufacturer's instructions, and the samples were stored at -80 °C. One microgram of total RNA was used to synthesize cDNA by the Transcriptor First Strand cDNA Synthesis kit (04897030001, Roche). Quantitative PCRs were performed with FastStart Essential DNA Green Master Mix (06924204001, Roche) on a LightCycler 96 Real-Time System (Roche). The primers used in the qPCR analysis are shown in Supplementary Table 4. Each reaction was performed in triplicate. A fragment of Gapdh was amplified as the internal control. Differences in gene expression were calculated by the $2^{-\Delta\Delta CT}$ method and are presented as the relative fold change.

Western blot analysis

Brain samples were lysed in RIPA lysis buffer with protease inhibitor cocktail (B14001, Bimake) by a tissue homogenizer, which was followed by ultrasonication and centrifugation. The bicinchoninic acid method was used to determine the protein concentrations, and proteins were mixed with 5× Laemmli sample buffer and denatured for 5 min at 95 °C. A total of 30 μg of each sample was separated by 8% sodium dodecyl sulfate-polyacrylamide gel electrophoresis (SDS-PAGE) and then transferred onto nitrocellulose membranes. Then, the membrane was incubated in blocking buffer (TBST buffer containing 5% skim milk powder) for 60 min at room temperature. Next, the membranes were incubated overnight at 4 °C with the primary antibodies. Primary antibodies were as follows: anti-FTO (1:1000, ab92821, Abcam), anti-Adrb2 (1:1000, ab182136, Abcam), anti-Sirt1 (1:1000, 8469S, Cell Signaling Technology), anti-c-Myc (9402S, 1:1000, Cell Signaling Technology), and anti-GAPDH (1:10000, GTX100118, GeneTex), anti Rabbit (1:5000, GTX213110-01,GeneTex), and anti-Mouse (1:5000, GTX213111-01 , GeneTex). After incubation for 1 h with the corresponding secondary antibodies, the protein bands were detected by chemiluminescence using an ECL reagent.

Stereotaxic surgery

Ten-week-old male mice were stereotaxically injected with rAAVs. Mice were anesthetized with 0.7% pentobarbital sodium via i.p. One microliter of rAAV per side was microinjected bilaterally into the hippocampus (2.2 mm posterior to bregma, 2.1 mm lateral to midline, and 1.7 mm dorsal to bregma) at a rate of 300 nanoliters/min with a Micro4 Syringe Pump Controller (World Precision Instruments, USA). Four weeks later, further experiments were performed.

m^{6}A Dot blot

Total RNA in 3 sample volumes of RNA incubation solution was denatured at 65 ℃ for 5 min and immediately chilled on ice. RNA samples were spotted in triplicate onto an Amersham Hybond-N+ membrane (RPN119B, GE Healthcare) with a Bio-Dot Apparatus (#170-6545, Bio-Rad). Next, they were crossed-linked to the membrane by UV light and then blocked with blocking buffer (PBST buffer containing 5% nonfat milk). The membrane was incubated overnight at 4 °C with anti-m^{6}A antibody (1:5000, 202003, Synaptic Systems) followed by incubation with HRP-conjugated goat anti-rabbit IgG (1:5000, sc-2030, Santa Cruz Biotechnology) for one hour at room temperature. Finally, the signal was detected by a chemiluminescent reaction using an ECL reagent.

MeRIP-seq

A refined MeRIP-Seq (N6-methyladenosine (m^{6}A) RNA immunoprecipitation sequencing) method was performed based on a previously described protocol[49,50]. The hippocampus was dissected from 3 mice, and the tissues were pooled together to obtain a sufficient quantity of mRNA for immunoprecipitation followed by RNA sequencing. Briefly, poly-A-purified RNA was extracted and randomly fragmented into approximately 100-200 nucleotide-long fragments. After enriching for methylated RNA fragments with a specific anti-m^{6}A antibody (1:100, ABE572, Millipore), the m6A-seq library was constructed using the SMARTer Stranded Total RNA-Seq Kit-v2 (Pico Input Mammalian, 634413, Takara/Clontech, Japan) and sequenced on Illumina Novaseq 6000.

Bioinformatics analysis of high-throughput sequencing data

Alignment. Sequencing data were analyzed according to the optimized pipeline for refined MeRIP-Seq described in a previous study[50]. The quality control of raw data was performed by FASTQC (version 0.11.5). The clean reads from the m^{6}A IP (m^{6}A-seq) were aligned to the mouse genome (mm10) using the STAR aligner (version 2.7) with the default parameters after removing reads containing adapters and low-quality reads with cutadapt (version 1.18). Only uniquely mapped and unduplicated reads remained for the subsequent analysis.

m^{6}A peak calling and motif analysis. MeTPeak (version 1.1) with the default settings was used for the transcriptome-wide detection of m6A sites in each sample based on the alignment files generated by STAR aligner. The R package Guitar was used to illustrate the distribution of m6A peaks in mRNA[51]. The top 3000 peaks were selected for motif analysis with DREME (version 5.1.1), which used 100-nt-long peak

summit-centered sense sequences as input. Peaks were annotated to overlapping genomic features and visualized with ChIPseeker (version 1.22.1) using annotations from TxDb.Mmusculus.UCSC.mm10.knownGene. Peaks were assigned to seven regions, including the promoter, 5’ UTR, 3’ UTR, exon, intron, and downstream and distal intergenic regions.

Detection of differential methylation peaks (DMPs). DMPs were identified according to the pipeline described in the four groups included in our study, including wild-type (WT), KD, cKO and OE mice. The following steps were taken to identify DMPs between three groups based on the expression levels in Fto-modified and control samples (WT mice). First, the overlapping m^6A peaks from two samples were defined as common peaks. The common peaks between samples from the same group were merged and combined with the common peaks from another group to form the m^6A union peaks reference list. Then, the read counts for the union peaks for the IP and input samples were calculated separately and corrected based on the total number of ERCC spike-in reads. The enrichment score of each sample for each peak was obtained by dividing the read counts for IP by the input. High confidence DMPs meeting the criteria of an average enrichment score higher than 6 in the groups and a log2 fold change > 1 or < −1 were selected for further analysis. The DMPs were annotated according to the genomic features with ChIPseeker (version 1.22.1)[52]. Functional enrichment analysis of the gene ontology (GO) and pathways was performed using ChIPseeker (version 1.22.1) to identify the predominant biological functions of the annotated genes nearest to the DMPs. Fisher’s exact test was applied to identify the significant GO categories and pathways, and FDR correction was performed with a threshold of 0.05.

Gene-specific m^6A qPCR

The Magna MeRIP m^6A kit (17-10499, Millipore) was used to perform m^6A RNA immunoprecipitation according to the manufacturer’s instructions. A QuantiTect SYBR Green RT-PCR Kit (204243, Qiagen) was used to perform reverse transcription and real-time qPCR. The relative expression of the m^6A-modified target gene was determined as the Cq value of the m^6A IP portion divided by the Cq value of the input portion.

RNA stability

Neuro-2a cells were transfected with *Fto*-shRNA and *Fto* overexpression and control vectors. Forty-eight hours later, the cells were treated with 5 μg/ml actinomycin D (A9415, Sigma) and harvested at 0, 3 and 6 h. Total RNA was extracted using TRIzol, and 1 μg of total RNA was used for reverse transcription and qPCR.

Golgi staining

Mice were anesthetized with chloral hydrate (10%, wt/vol, i.p.) and sequentially perfused transcardially with saline. The whole brain was freshly harvested and was immediately immersed in one well of a 12-well plate containing 5 ml of solution A (superGolgi Kit, Cat. # 003010, Bioenno Tech, LLC). According to the manufacturer’s instructions, the solution was renewed two days later, and the impregnation continued

for another 9 days. Next, the brain was transferred to postimpregnation buffer for 2 days with renewal of the solution after one day of immersion. Sections that were 100 μm in thickness were cut using a vibratome (VT1200S, Leica). The sections were mounted on adhesive microscope slides (SUPERFROST® PLUS, Cat. # 4951 PLUS-100E, Thermo Scientific). The staining time in solutions C and D was 20 min. Then, the sections were dehydrated in 100% ethanol for 7 min 4 times each, which was followed by vitrification with xylene for 8 min 10 times each. Finally, the sections were coverslipped with neutral resins. For spine density measurement, we imaged one terminal dendrite from the CA1 region of the hippocampus using a 100× objective on a microscope (DM6 B, Leica). A Z-stack of images with an interval of 0.22 μm was acquired for each dendritic segment, which was followed by an extended depth of field algorithm calculation to obtain in focus images using LAS X software (Leica Application Suite X, Leica). The diameters of the selected segments were comparable. A total of 120 segments from 20 mouse brains (6 segments per animal) were used to determine the spine number. The dendritic spines, including thin, stubby, and mushroom types, within a 15-μm length segment were counted manually by an investigator blinded to the experimental treatments.

Statistical analysis

Statistical significance was analyzed with Prism software (GraphPad Prism 8). Two-tailed student's t test was used for comparisons between the two groups, and one-way or two-way ANOVA was performed for more than two groups. $P < 0.05$ was considered statistically significant. All the data were exported into Adobe Photoshop CS6 for the preparation of figures. All data are shown as the mean ± s.e.m.

Additional Information

Reporting summary.

Further information on research design is available in the Nature Research Reporting Summary linked to this article.

Data availability

Correspondence and requests for materials should be addressed to DBPR (manuscript NCOMMS-21-04052).

References

1. Otte, C. et al. Major depressive disorder. *Nat Rev Dis Primers.* **2**, 16065 (2016).
2. Binder, E. B. Dissecting the molecular mechanisms of gene x environment interactions: implications for diagnosis and treatment of stress-related psychiatric disorders. *Eur J Psychotraumatol.* **8**, 1412745 (2017).
3. Pena, C. J. & Nestler, E. J. Progress in Epigenetics of Depression. *Prog Mol Biol Transl Sci.* **157**, 41–66 (2018).

4. Livneh, I., Moshitch-Moshkovitz, S., Amariglio, N., Rechavi, G. & Dominissini, D. The m(6)A epitranscriptome: transcriptome plasticity in brain development and function. *Nat. Rev. Neurosci.* **21**, 36–51 (2020).
5. Meyer, K. D. et al. Comprehensive analysis of mRNA methylation reveals enrichment in 3' UTRs and near stop codons. *Cell.* **149**, 1635–1646 (2012).
6. Yang, Y., Hsu, P. J., Chen, Y. S. & Yang, Y. G. Dynamic transcriptomic m(6)A decoration: writers, erasers, readers and functions in RNA metabolism. *Cell Res.* **28**, 616–624 (2018).
7. Gerken, T. et al. The obesity-associated FTO gene encodes a 2-oxoglutarate-dependent nucleic acid demethylase. *Science.* **318**, 1469–1472 (2007).
8. Gao, X. et al. The fat mass and obesity associated gene FTO functions in the brain to regulate postnatal growth in mice. *PLoS One.* **5**, e14005 (2010).
9. Hess, M. E. et al. The fat mass and obesity associated gene (Fto) regulates activity of the dopaminergic midbrain circuitry. *Nat. Neurosci.* **16**, 1042–1048 (2013).
10. Widagdo, J. et al. Experience-Dependent Accumulation of N6-Methyladenosine in the Prefrontal Cortex Is Associated with Memory Processes in Mice. *J. Neurosci.* **36**, 6771–6777 (2016).
11. Engel, M. et al. The Role of m6A/m-RNA Methylation in Stress Response Regulation. *Neuron.* **99**, 389–403 (2018).
12. Li, L. et al. Fat mass and obesity-associated (FTO) protein regulates adult neurogenesis. *Hum. Mol. Genet.* **26**, 2398–2411 (2017).
13. Spychala, A. & Rüther, U. FTO affects hippocampal function by regulation of BDNF processing. *PLoS One.* **14**, e211937 (2019).
14. Walters, B. J. et al. The Role of The RNA Demethylase FTO (Fat Mass and Obesity-Associated) and mRNA Methylation in Hippocampal Memory Formation. *Neuropsychopharmacology: official publication of the American College of Neuropsychopharmacology.* **42**, 1502–1510 (2017).
15. Weng, Y. L. et al. Epitranscriptomic m(6)A Regulation of Axon Regeneration in the Adult Mammalian Nervous System. *Neuron.* **97**, 313–325 (2018).
16. Merkurjev, D. et al. Synaptic N(6)-methyladenosine (m(6)A) epitranscriptome reveals functional partitioning of localized transcripts. *Nat. Neurosci.* **21**, 1004–1014 (2018).
17. Yu, J. et al. Dynamic m6A modification regulates local translation of mRNA in axons. *Nucleic Acids Res.* **46**, 1412–1423 (2018).
18. Milaneschi, Y. et al. The effect of FTO rs9939609 on major depression differs across MDD subtypes. *Mol Psychiatry.* **19**, 960–962 (2014).
19. Samaan, Z. et al. The protective effect of the obesity-associated rs9939609 A variant in fat mass- and obesity-associated gene on depression. *Mol Psychiatry.* **18**, 1281–1286 (2013).
20. Rivera, M. et al. Depressive disorder moderates the effect of the FTO gene on body mass index. *Mol Psychiatry.* **17**, 604–611 (2012).

21. Sun, L. et al. *Fto* Deficiency Reduces Anxiety- and Depression-Like Behaviors in Mice via Alterations in Gut Microbiota. *Theranostics.* **9**, 721–733 (2019).
22. Dominissini, D. et al. Topology of the human and mouse m6A RNA methylomes revealed by m6A-sEq. *Nature.* **485**, 201–206 (2012).
23. Bortolotto, V. et al. Salmeterol, a beta2 Adrenergic Agonist, Promotes Adult Hippocampal Neurogenesis in a Region-Specific Manner. *Front Pharmacol.* **10**, 1000 (2019).
24. Dang, V. et al. Formoterol, a Long-Acting β2 Adrenergic Agonist, Improves Cognitive Function and Promotes Dendritic Complexity in a Mouse Model of Down Syndrome. *Biol. Psychiat.* **75**, 179–188 (2014).
25. Havekes, R. et al. Gravin Orchestrates Protein Kinase A and 2-Adrenergic Receptor Signaling Critical for Synaptic Plasticity and Memory. *J. Neurosci.* **32**, 18137–18149 (2012).
26. Li, S. et al. Environmental novelty activates beta2-adrenergic signaling to prevent the impairment of hippocampal LTP by Abeta oligomers. *Neuron.* **77**, 929–941 (2013).
27. Zhang, H., Huang, Y. & O'Donnell, J. M. Antagonism of the antidepressant-like effects of clenbuterol by central administration of β-adrenergic antagonists in rats. *Psychopharmacology.* **170**, 102–107 (2003).
28. Wang, X. et al. N6-methyladenosine-dependent regulation of messenger RNA stability. *Nature.* **505**, 117–120 (2014).
29. Duman, R. S. & Aghajanian, G. K. Synaptic dysfunction in depression: potential therapeutic targets. *Science.* **338**, 68–72 (2012).
30. Gao, J. et al. A novel pathway regulates memory and plasticity via SIRT1 and miR-134. *Nature.* **466**, 1105–1109 (2010).
31. Michan, S. et al. SIRT1 is essential for normal cognitive function and synaptic plasticity. *J. Neurosci.* **30**, 9695–9707 (2010).
32. Abe-Higuchi, N. et al. Hippocampal Sirtuin 1 Signaling Mediates Depression-like Behavior. *Biol Psychiatry.* **80**, 815–826 (2016).
33. Chen, H. et al. beta2-AR activation induces chemoresistance by modulating p53 acetylation through upregulating Sirt1 in cervical cancer cells. *Cancer Sci.* **108**, 1310–1317 (2017).
34. Yuan, J., Minter-Dykhouse, K. & Lou, Z. A c-Myc-SIRT1 feedback loop regulates cell growth and transformation. *J. Cell Biol.* **185**, 203–211 (2009).
35. Branca, C., Wisely, E. V., Hartman, L. K., Caccamo, A. & Oddo, S. Administration of a selective beta2 adrenergic receptor antagonist exacerbates neuropathology and cognitive deficits in a mouse model of Alzheimer's disease. *Neurobiol. Aging.* **35**, 2726–2735 (2014).
36. O'Donnell, J. M. Behavioral consequences of activation of beta-adrenergic receptors by clenbuterol: evidence for mediation by the central nervous system. *Brain Res. Bull.* **21**, 491–497 (1988).
37. Cai, N et al. Sparse whole-genome sequencing identifies two loci for major depressive disorder. *Nature.* **523**, 588–591 (2015).

38. Luo, X. J. & Zhang, C. Down-Regulation of SIRT1 Gene Expression in Major Depressive Disorder. *Am J Psychiatry.* **173**, 1046 (2016).
39. Kim, H. D. et al. SIRT1 Mediates Depression-Like Behaviors in the Nucleus Accumbens. *J. Neurosci.* **36**, 8441–8452 (2016).
40. Lei, Y. et al. SIRT1 in forebrain excitatory neurons produces sexually dimorphic effects on depression-related behaviors and modulates neuronal excitability and synaptic transmission in the medial prefrontal cortex. *Mol Psychiatry*, (2019).
41. Lu, G. et al. Role and Possible Mechanisms of Sirt1 in Depression. *Oxid. Med. Cell. Longev.* 2018, 1–6 (2018).
42. Menssen, A. et al. The c-MYC oncoprotein, the NAMPT enzyme, the SIRT1-inhibitor DBC1, and the SIRT1 deacetylase form a positive feedback loop. *Proceedings of the National Academy of Sciences*. **109**, E187-E196 (2012).
43. Su, R. et al. Targeting FTO Suppresses Cancer Stem Cell Maintenance and Immune Evasion. *Cancer Cell.* **38**, 79–96 (2020).
44. Peng, S. et al. Identification of entacapone as a chemical inhibitor of FTO mediating metabolic regulation through FOXO1. *Sci. Transl. Med.* **11**, (2019).
45. Liu, C., Lee, S. & Elmquist, J. K. Circuits controlling energy balance and mood: inherently intertwined or just complicated intersections? *Cell Metab.* **19**, 902–909 (2014).
46. Liu, S. et al. Inverse changes in L1 retrotransposons between blood and brain in major depressive disorder. *Sci Rep.* **6**, 37530 (2016).
47. Haenisch, B., Bilkei-Gorzo, A., Caron, M. G. & Bonisch, H. Knockout of the norepinephrine transporter and pharmacologically diverse antidepressants prevent behavioral and brain neurotrophin alterations in two chronic stress models of depression. *J. Neurochem.* **111**, 403–416 (2009).
48. Golden, S. A., Covington, H. R., Berton, O. & Russo, S. J. A standardized protocol for repeated social defeat stress in mice. *Nat. Protoc.* **6**, 1183–1191 (2011).
49. Dominissini, D., Moshitch-Moshkovitz, S., Salmon-Divon, M., Amariglio, N. & Rechavi, G. Transcriptome-wide mapping of N(6)-methyladenosine by m(6)A-seq based on immunocapturing and massively parallel sequencing. *Nat. Protoc.* **8**, 176–189 (2013).
50. Zeng, Y. et al. Refined RIP-seq protocol for epitranscriptome analysis with low input materials. *PLoS Biol.* **16**, e2006092 (2018).
51. Cui, X. et al. Guitar: An R/Bioconductor Package for Gene Annotation Guided Transcriptomic Analysis of RNA-Related Genomic Features. *Biomed Res. Int.* 2016, 8367534 (2016).
52. Yu, G., Wang, L. G. & He, Q. Y. ChIPseeker: an R/Bioconductor package for ChIP peak annotation, comparison and visualization. *Bioinformatics.* **31**, 2382–2383 (2015).

Figures

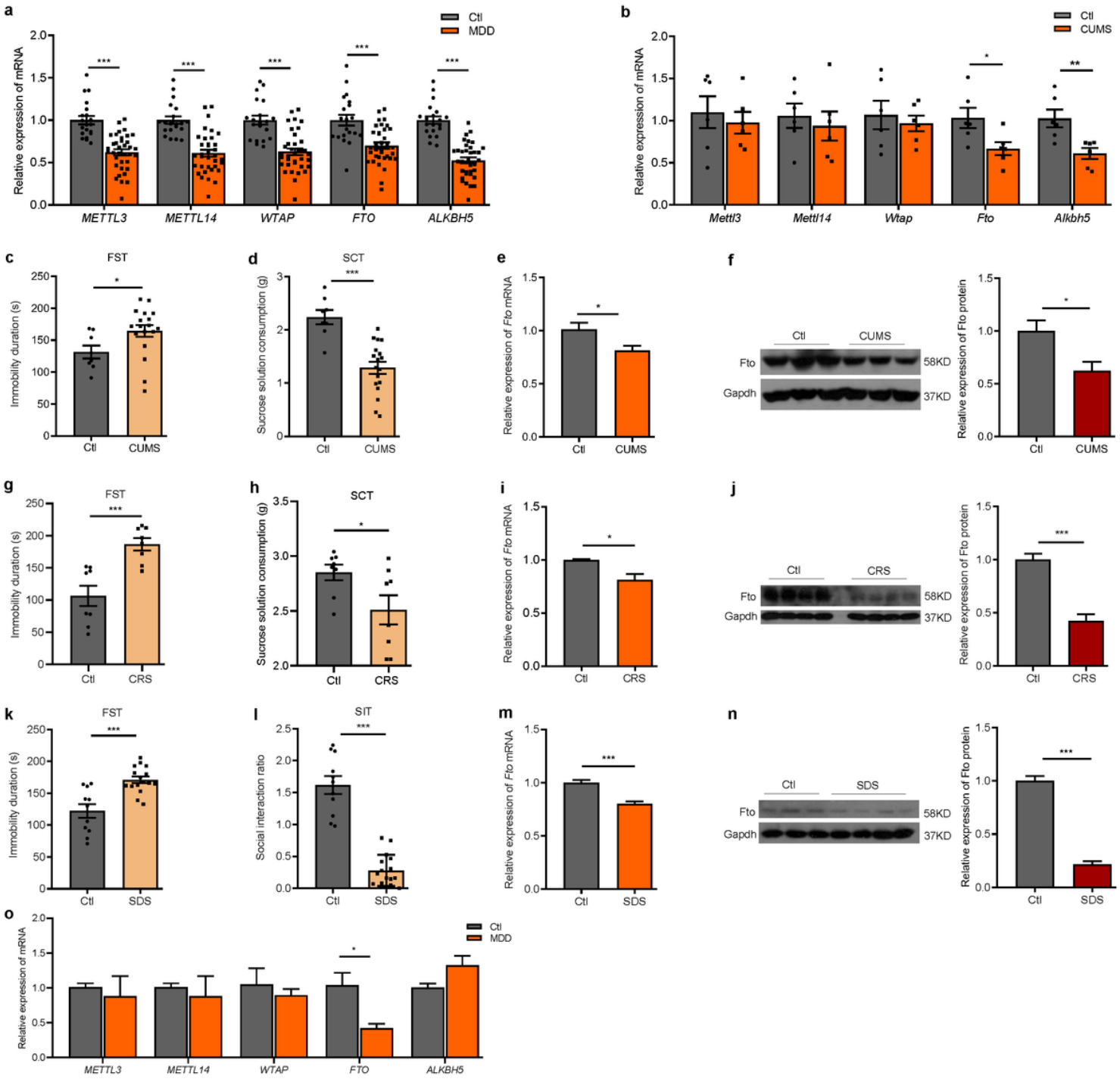

Figure 1

Expression of FTO is decreased in the hippocampi of MDD patients and mouse models of depression. a Microarray analysis of genes encoding m6A-modifying enzymes in the peripheral blood of humans. Ctl, n = 20; MDD, n = 36. b mRNA expression of m6A-modifying enzymes in the peripheral blood of mice, n = 6 per group. CUMS, chronic unpredictable mild stress. c, d Forced swimming test (FST) and sucrose consumption test (SCT) in the CUMS mouse model. Ctl, n = 8; CUMS, n = 18. e Expression of hippocampal Fto mRNA in the CUMS model. n = 8 per group. f Expression of hippocampal Fto protein in the CUMS model. n = 3 per group. g, h FST and SCT in the chronic restraint stress (CRS) mouse model. n

= 8 per group. i Expression of hippocampal Fto mRNA in the CRS model. Ctl, n = 3; CRS, n = 4. j Expression of hippocampal Fto protein in the CRS model. n = 4 per group. k, l FST and social interaction test (SIT) in the social defeat stress (SDS) mouse model. Ctl, n = 11; SDS, n = 15. m Expression of hippocampal Fto mRNA in the SDS model. n = 4 per group. n Expression of hippocampal Fto protein in the SDS model. Ctl, n = 3; SDS, n = 4. o mRNA expression of m6A-modifying enzymes in the hippocampi of MDD patients. n = 3 per group. *p < 0.05, ***p < 0.001. Two-tailed student's t-test. Error bars represent s.e.m.

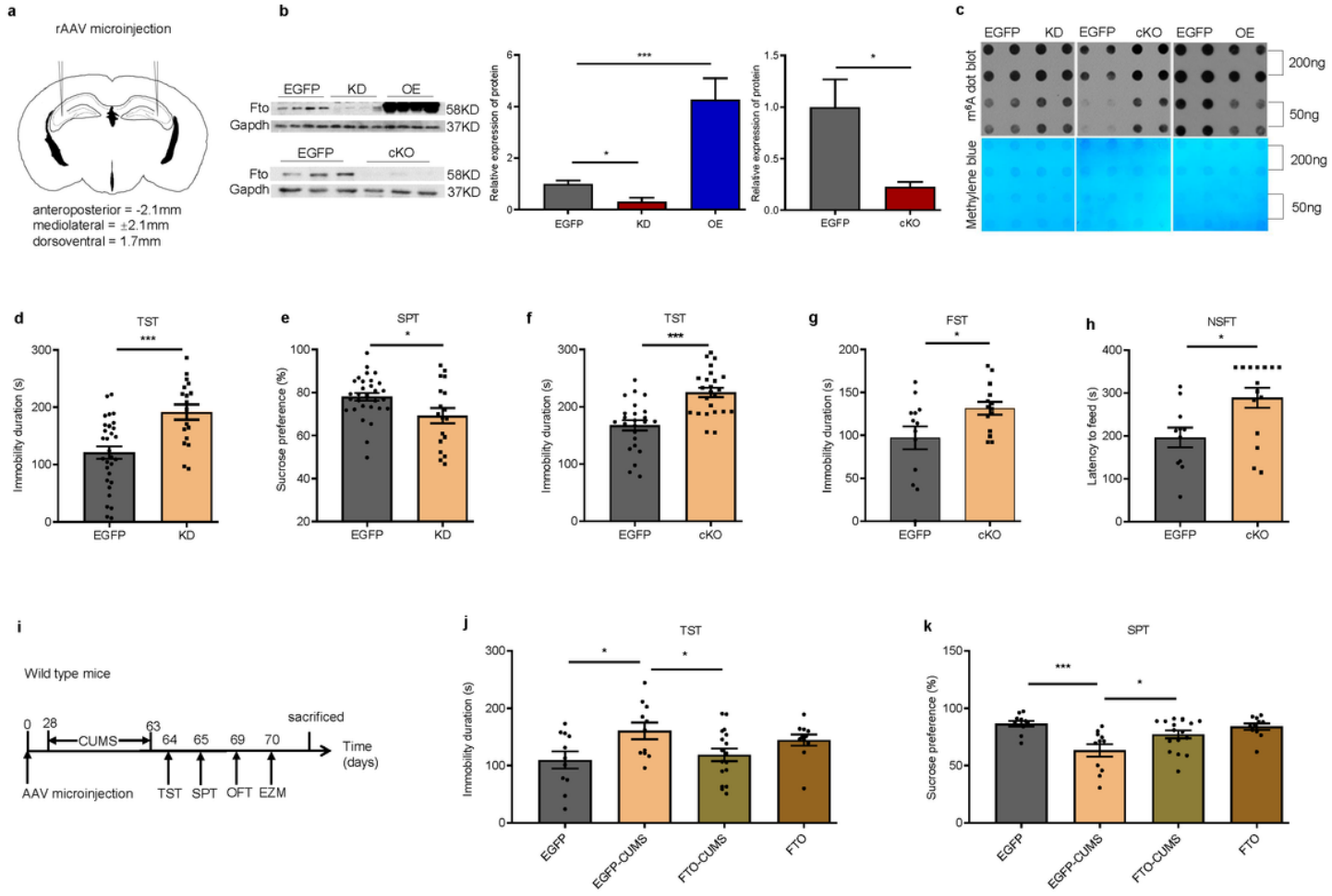

Figure 2

Fto in the hippocampus mediates depression-like behaviors. a Schematics illustrating rAAV microinjection. b Knockdown (KD), overexpression (OE), and knockout (cKO) of Fto in the hippocampus. EGFP, KD, OE, n = 4 per group; EGFP, cKO, n = 3 per group. c m6A dot blot assay of hippocampal total RNA. d, e Tail suspension test (TST) and sucrose preference test (SPT) in KD mice. Ctrl, n = 31; KD, n = 18. f-h TST, FST, and novelty suppressed feeding test (NSFT) in three cohorts of cKO mice. (f) n = 24 per group; (g) EGFP, n = 13; cKO, n = 14; (h) EGFP, n = 11; cKO, n = 15. i Schematics of the experimental design. j, k TST and SPT in OE mice subjected to CUMS. EGFP, EGFP-CUMS, FTO, n = 11 per group; FTO-CUMS, n = 17. *p < 0.05, ***p < 0.001. Two-tailed student's t-test for b & d-h; one-way analysis of variance for j & k. Error bars represent s.e.m.

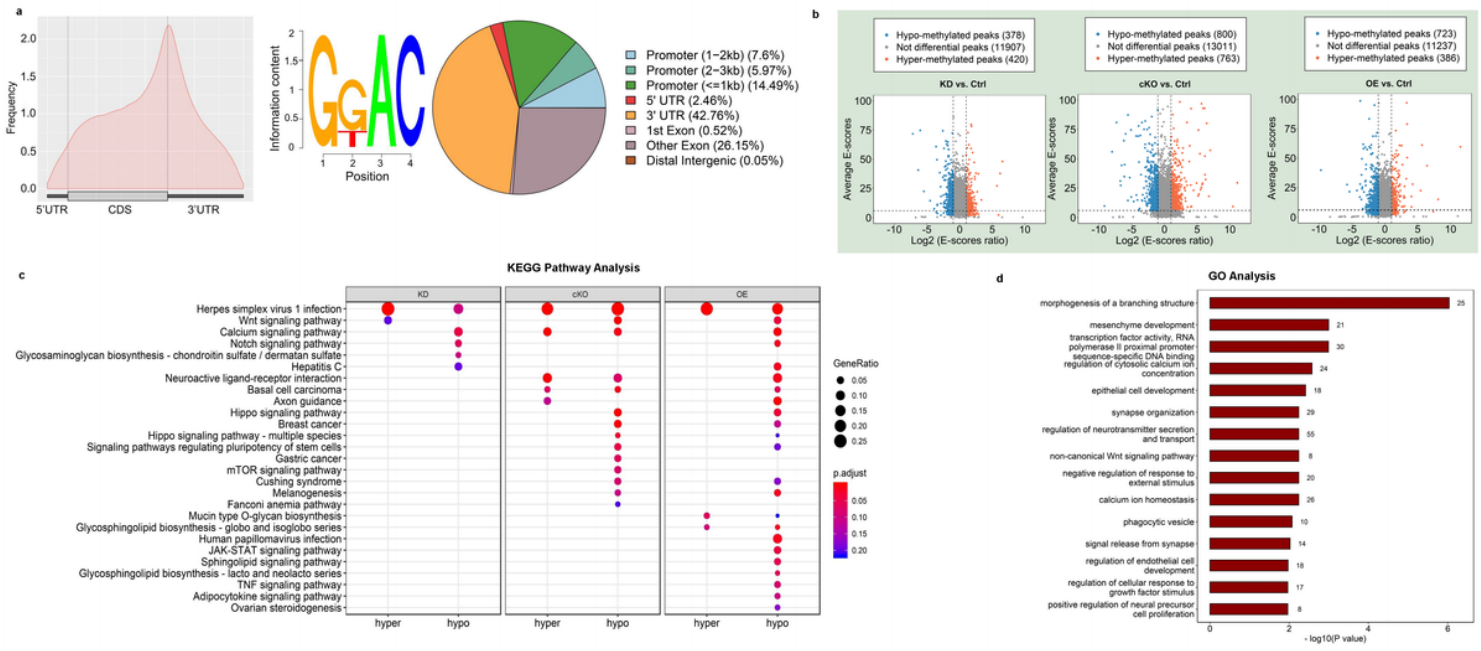

Figure 3

Hippocampal m6A epitranscriptome modified by Fto. a Left: distribution of m6A peaks throughout the whole mRNA transcript; middle: the most abundant motifs detected in peaks and enriched at peak summits; right: annotation of peaks detected in cKO mice. b Differentially methylated peaks among different groups. c KEGG pathway analysis of differentially methylated genes in different groups. d GO (gene ontology) analysis of genes with hypomethylated peaks in OE mice.

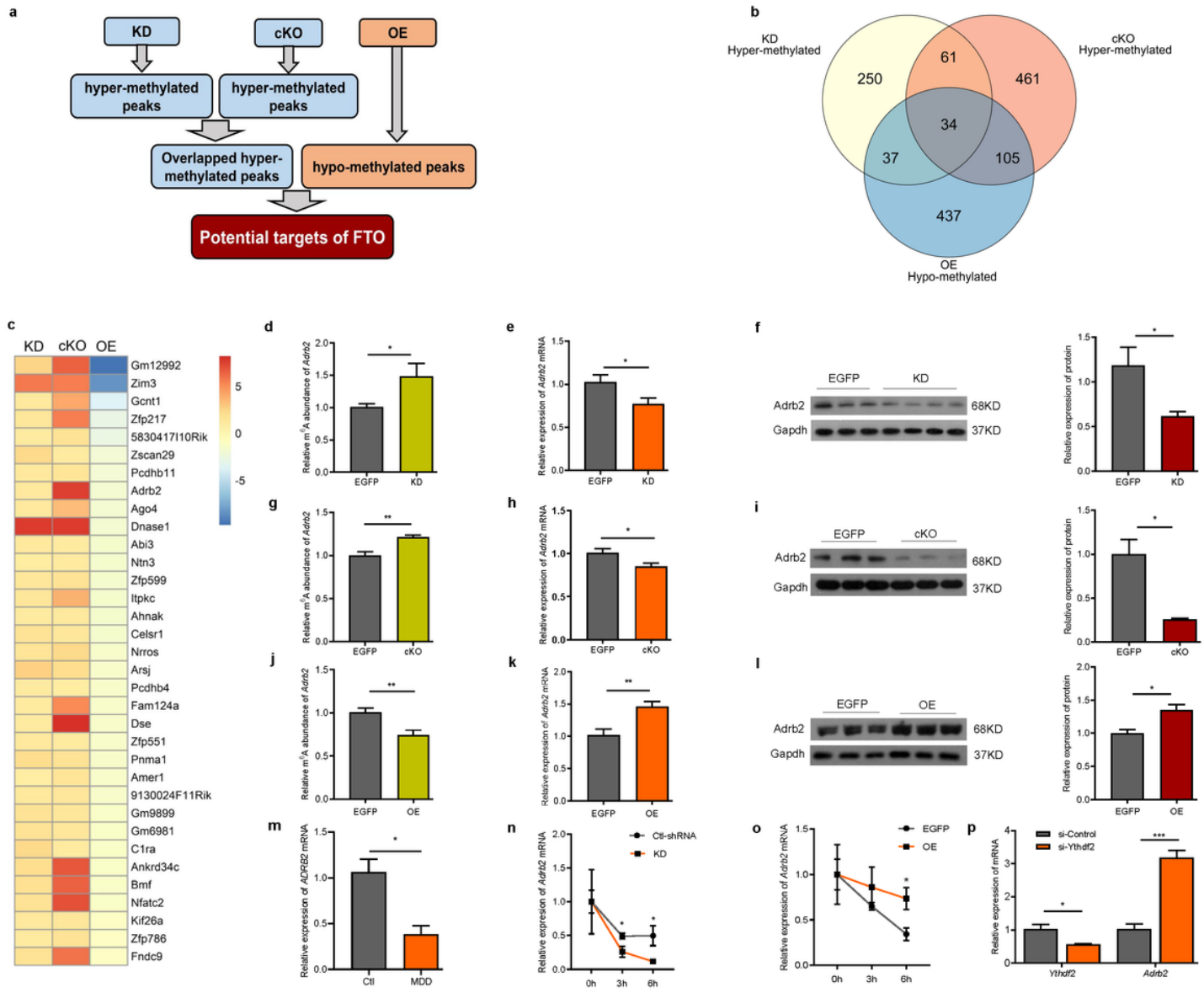

Figure 4

Adrb2 is one of critical target genes of FTO in the hippocampus. a Schematics of the strategy used to identify the targets. b Overlap of genes that are hypermethylated in KD and cKO mice and hypomethylated in OE mice. c Thirty-four genes that are hypermethylated in KD and cKO mice and hypomethylated in OE mice. d-l m6A, mRNA, and protein levels of Adrb2 in the hippocampus of KD (d-f) cKO (g-i) and OE (j-l) mice. (d) n = 6 per group; (e) n = 8 per group; (f) EGFP, n = 3; KD, n = 4; (g) EGFP, n = 5; cKO, n = 6; (h) EGFP, n = 7; cKO, n = 6; (i) n = 3 per group; (j, k) n = 8 per group; (l) n = 3 per group. m Expression of Adrb2 mRNA in the hippocampi of MDD patients and healthy controls. n = 3 per group. n, o Adrb2 mRNA stability assay after transfection of Neuro-2a cells with plasmids expressing Fto-shRNA or Fto. n = 4 per time point. p Levels of Ythdf2 and Adrb2 mRNA after knockdown of Ythdf2 in Neuro-2a cells. n = 4 per group. *p < 0.05, **p < 0.01, ***p < 0.001. Two-tailed student's t-test for d-m & p; two-way ANOVA with repeated measures followed by post hoc Tukey's test for n & o. Error bars represent s.e.m.

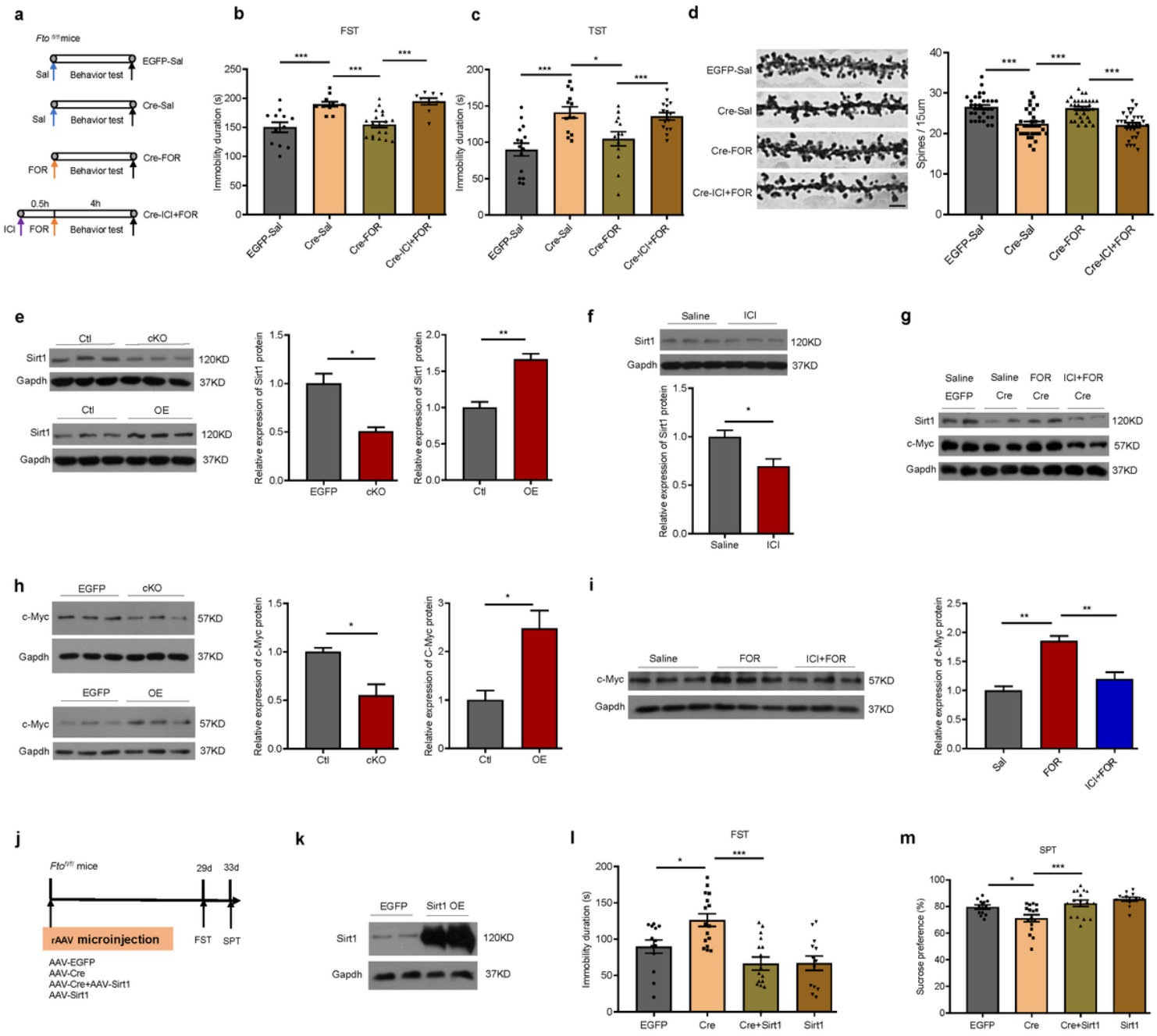

Figure 5

Adrb2 stimulation rescues depression-like behaviors and spine loss induced by hippocampal Fto deficiency. a Schematics of the experimental design. Sal, Saline; FOR, formoterol, a specific Adrb2 agonist; ICI, ICI 118,551, a specific Adrb2 antagonist. b FST in one cohort of cKO mice. EGFP-Sal, n = 12; Cre-Sal, n = 11; Cre-FOR, n = 19; Cre-ICI+FOR, n = 9. c TST in the other cohort of cKO mice. EGFP-Sal, n = 15; Cre-Sal, n = 13; Cre-FOR, n = 13; Cre-ICI+FOR, n = 15. d Spine density analysis in the hippocampi of cKO mice after seven days of Adrb2 stimulation. n = 30 per group. Scale bar = 2 μm. e Sirt1 expression in the hippocampi of cKO and OE mice. n = 3 per group. f Sirt1 expression in the hippocampi of wild-type mice treated with ICI or saline for 4.5 h. n = 3 per group. g Sirt1 and c-Myc expression in the hippocampi of cKO and control mice after Adrb2 stimulation. h c-Myc expression in the hippocampi of cKO and OE

mice. n = 3 per group. i c-Myc expression in the hippocampi of wild-type mice after Adrb2 stimulation. n = 3 per group. j Schematics of the experimental design. k Sirt1 overexpression in the hippocampus. l, m FST and SPT after elevation of Sirt1 expression in the hippocampi of cKO and control mice. EGFP, n = 13; Cre, n = 16; Cre+Sirt1, n = 16; Sirt1, n = 13. *p < 0.05, **p < 0.01, ***p < 0.001. Two-tailed student's t-test for e & h; one-way analysis of variance for b-d, f, i, l, and m. Error bars represent s.e.m.

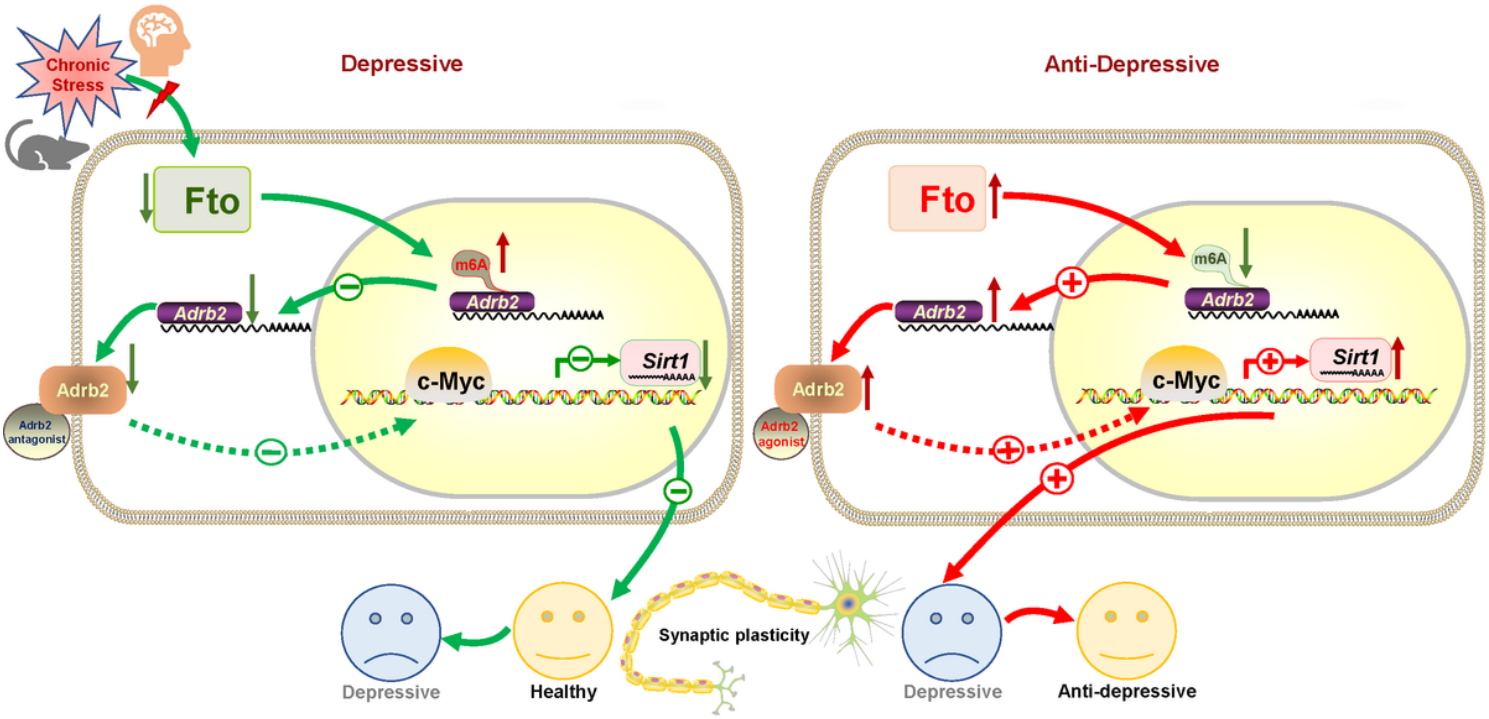

Figure 6

Scheme summarizing Fto-mediated depression-like behaviors in the hippocampus. Expression of hippocampal FTO is decreased in both MDD patients and stress-induced mouse models of depression. Downregulation of Fto leads to elevated levels of m6A modification of Adrb2 mRNA, which results in lower mRNA and protein levels of Adrb2, whereas enhancing Fto expression in the hippocampus of mice exposed to CUMS reduced m6A modification of Adrb2 mRNA, which results in higher mRNA and protein levels of Adrb2. Adrb2 stimulation reverses the depression-like behaviors and spine loss induced by Fto deficiency, possibly through the regulation of Sirt1 expression by c-Myc. The picture material was downloaded from ScienceSlides (http://www.scienceslides.com).

Supplementary Files

This is a list of supplementary files associated with this preprint. Click to download.

- SupplementaryInformation.pdf